Design of the ITER Magnets to Provide Plasma Operational Flexibility

N. Mitchell, D. Bessette, M. Ferrari, M. Huguet, C. Jong, Y. Takahashi, K. Yoshida 1)
R. Maix 2)
Y. Krivchenkov, E. Zapretilina 3)

1) ITER IT, Naka and Garching JWS
2) ATI Atominstitut Wien, Austria
3) Efremov Institute, St. Petersburg, Russia

email contact of main author mitchen@itergps.naka.jaeri.go.jp

Abstract. The ITER magnets have been optimised and refined since the ITER Final Design Report (FDR) in 2001. Multiple design options have been eliminated and there is improved ability to drive a wide range of plasma configurations. Design iterations on the TF out of plane supports have eliminated stress concentrations in the inner keyways and have led to the choice of a so called friction-joint on the outside. The closure procedure for the TF case has been changed, with a new case segmentation, less risk of winding pack damage from shrinkage and better filling of the case-winding gaps. Selection of compact joints for the CS has enabled the peak field and cyclic stress levels in the conductor to be reduced while maintaining the flux capability. The uncertainty in the nuclear heat levels in the inner legs of the TF coils, and the need to operate with plasma nuclear powers from 360 to 700MW, lead to a thermal screen on the inside of the case with variable cooling capability. The electrical insulation specification has been refined after irradiation test results to give a better margin on the onset of degradation after operation to 3MWa/m^2. The RWM stabilisation provided by the side CC has been extended by accepting higher voltages and heating from AC losses. R&D results from the model coil tests have shown lower than expected design margins for the Nb3Sn conductors. This has been offset by adopting the latest advances in strand performance, and the margins of the new conductor will be confirmed by testing in 2005. Preparation for procurement is underway with considerations on technically acceptable ways of splitting the magnet supply.

1. Introduction

The ITER Magnets, consisting of the Toroidal Field (TF), Central Solenoid (CS), Poloidal Field (PF) and Correction Coil (CC) coil systems, have undergone design optimisation and refinement, improving their ability to drive a wide range of plasma configurations. The design in 2001 had a significant number of open options, major ones being 3 conductor/layouts for the CS, 2 for the TF and 2 concepts for the TF structures, to the extent that preparation of manufacturing specifications was being hindered due to design uncertainty. Detailed investigations and negotiations with the ITER partners have now reduced this to a single agreed reference design. At the same time, detailed design and analysis, in particularly the inner poloidal key region, in the TF cooling and nuclear shielding and the CCs, has improved the functionality of the design to accommodate a range of plasmas without significantly affecting the cost or the overall machine parameters

As defined in 2001, the coils use low temperature superconductors cooled with supercritical helium at about 5K, Nb3Sn for the TF (11.8T) and CS (13T) and NbTi for the PF (6T) and CC (3.4T). The cables are multistage cable in conduit type, with up to 1200 strands. The TF coils are arranged in a wedged configuration, with a free standing CS (subdivided into 6 independent modules) within the central vault. The TF coils are supported by cases and toroidal links of Outer Intercoil Structures (OIS), the CS and PF coils are supported by the thick conductor jacket. All coils use glass-kapton insulation vacuum impregnated with epoxy resin.

In the following sections, both the reduction of design options and the improvement of the design functionality are discussed in more detail [1].

2. Structural Design

Pulsed plasma operation creates fatigue in the magnet structural elements, a particular issue for large metallic structures which inevitably contain manufacturing defects that act as crack initiators, especially within welds. Optimisation of the TF out of plane supports has eliminated stress concentrations in the inner keyways and led to the choice of a so called 'friction-joint' on the outside, minimising interference with the plasma access ducts. Fig 1 shows main case sub assemblies and the inner poloidal key arrangement with shortened keyways at lower radius to give a uniform load transmission.

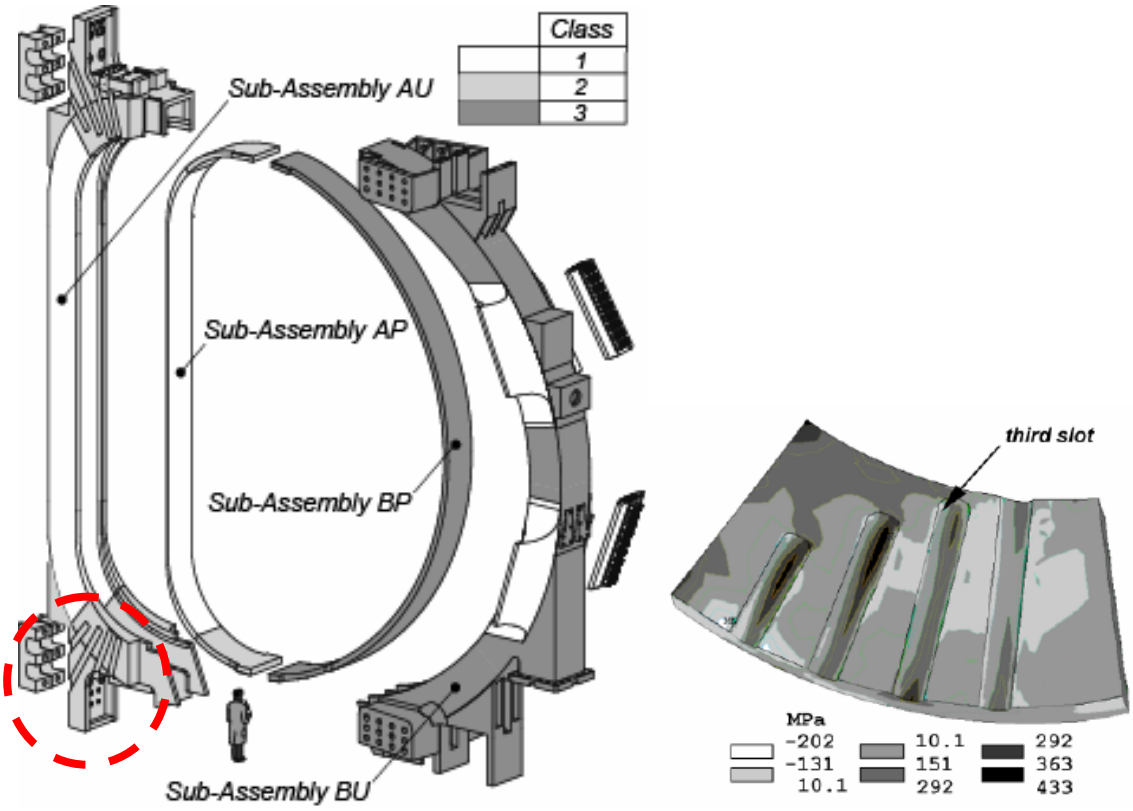

Fig 1 TF Coil Case Segmentation, Material Classes and Stress Analysis of Inner Poloidal Keyways (Showing Maximum Principal Stress at EOB)

Mechanical R&D for the coils has consisted of characterisation of cryogenic steels, welding development and fabrication of large representative forged sections. Major items were successfully complete before 2001 but characterisation and welding development is continuing. The results have led to a redefinition of the property requirements of the TF structures since 2001, subdividing the material into 3 grades depending on the location, minimising the quantity of the highest (and most expensive) grade with guaranteed yield stress >1000MPa at 4K to 25% of the total weight of 207t, as shown in Fig 1. The lowest grade 3 requires a guaranteed yield stress >750MPa at 4K, and makes up 45% of the weight.

The insertion of the winding pack into the case has been changed. Sub-assembly AU is placed horizontally and the winding pack (as a complete unit with ground insulation) is lowered into the nose 'U' part. This achieves a near perfect match of the nose region (which carries the highest winding pack-case stress). The side gaps are filled with compressed dry glass sheets (pre-attached to the winding) and the outer section BU is put over the upper part of the

winding. BU is then joined to AU by a butt weld (at a low stress location) and the inner cover plates AP, BP are put in place. These are welded without moving the coil (which would disturb the good fit at the nose). The dry glass around the winding allows weld shrinkage without damage and the case-winding pack gap is then vacuum impregnated with epoxy resin.

Selection of compact joints for the CS has enabled the peak field and cyclic stress levels in the conductor to be reduced (from 13.5 to 13T) while maintaining the poloidal flux capability. The selection of the optimum field for the CS coils involves a balance between superconductor current density (that decreases with increasing field) and the allowable operating stress (which requires more structure as the field increases). The coils become thicker as the field increases and the available flux reaches a maximum and then decreases, Fig 2 shows the optimisation for the ITER CS, with a peak stress of 400MPa. For comparison, half of the burn flux (the plot shows prebias flux so the total effect is doubled) is about 15Vs.

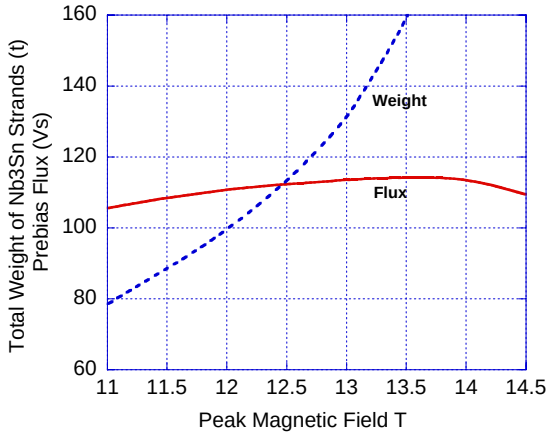

Fig 2: Flux Optimisation of the CS

The range of possible plasma internal inductance and beta (0.7-1.0 and 0.1-0.9 respectively at 15MA) that may occur in the inductive scenarios generate separating forces within the CS that require a robust vertical support structure, now designed to occupying a minimum of radial space outside the CS coils. Extensive optimisation of the supports, joints and the layout of the current and helium supplies to the individual CS modules has been performed, giving standardised identical modules for manufacture and improving the plasma shaping capability. A view of these is shown in Fig 3. The helium supplies make use of the inner bore to save space, with the outlets led through from the outside in the gaps between the modules.

3. Superconductor Design

Superconducting R&D was focused on the two model coils (CS Model Coil with its inserts and TF Model Coil). Assessment of the Nb3Sn cable performance from these has showed some discrepancies from those expected based on the performance of isolated Nb3Sn strands. This appears to be associated with transverse mechanical loads on the conductors (up to 40t/m). Testing is still underway to quantify the effect but it is clearly illustrated in recent results from EPFL-PSI [2], shown in Fig 4. Nb3Sn strands can show progressive filament fracture under overall tension [3] and to avoid this risk, a steel conductor jacket has been chosen as the reference (instead of Ti). This creates overall compression due to differential contraction but, as seen in Fig 4, the compression also results in lower strand performance.

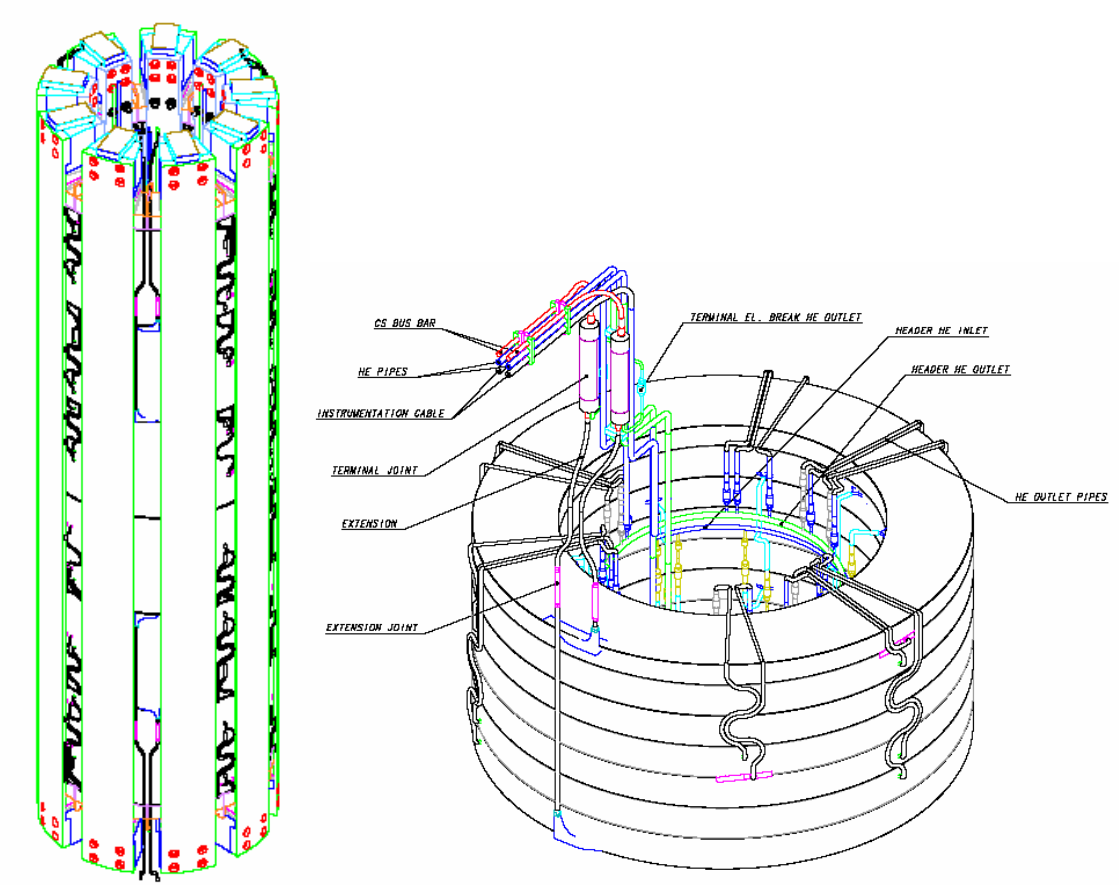

Fig 3 CS Overall Layout Showing Services Between Flanges and Use of Inner Bore

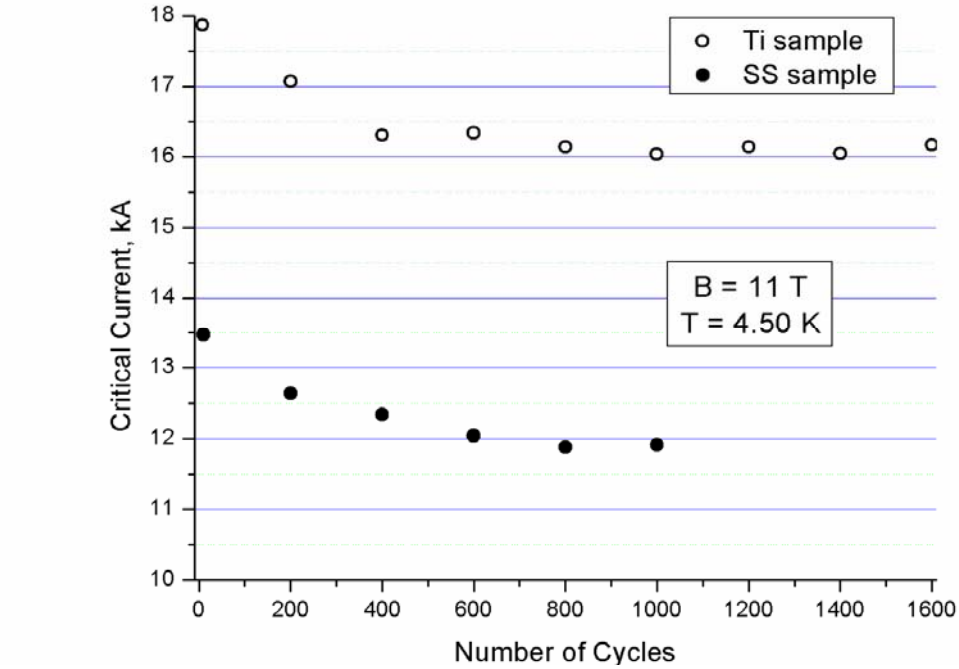

Fig 4 Behaviour of Nb3Sn Strands in a (Subsize, one sixth scale) Cable, Showing Initial Performance Drop in Critical Current Probably Caused by Cable Settlement (reproduced by permission from [2]). The Cable is Identical, with either a Steel or Ti Jacket Producing Different Thermal Strain on the Strands (difference equivalent to about 0.1 to 0.15% strain)

The performance drop requires some increase in temperature margin. This has been obtained without increasing the cable dimensions by taking advantage of recent improvements in the

technology of Nb3Sn strand production which has increased the critical current by over 20% compared to what was available at the start of the model coil procurement 8 years ago, Fig 5.

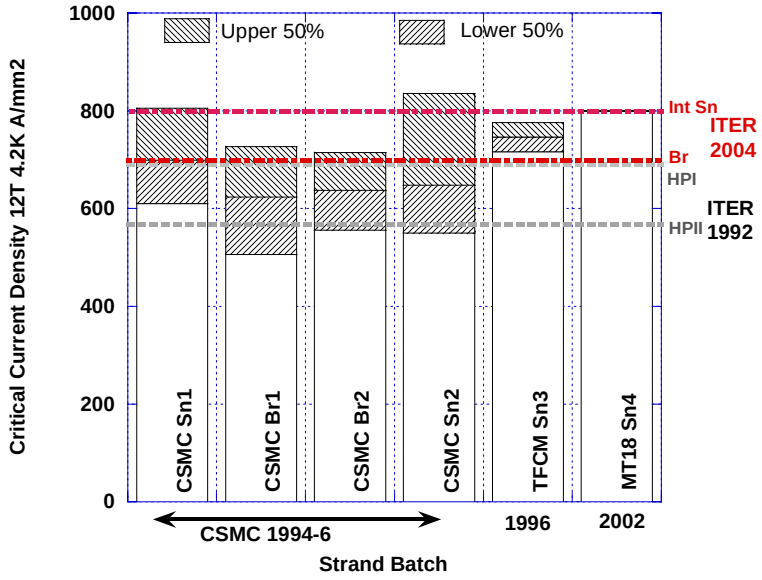

Fig 5 Improvements in Strand Performance During/Since Model Coil Construction, Range of Critical Current Compared to Specification (HPI and HPII are the original bronze/ internal tin specification, Br is bronze route, Sn is internal tin, MT18 is a published reference)

4. Cryogenic Design

The heat loads on the cryogenic system, both the various components and their variation over the main phases of the burn, are summarised in Fig 6. The mainly static loads from the current leads and thermal radiation are the largest part, at just over 50%. However most of this is external to the magnets and has no influence on their design. More important are the pulsed AC loss, eddy current and nuclear components. It is noticeable that the pumping power to remove these internal heat loads is as large as the heat loads themselves.

For the thermohydraulic design, the uncertainty of the calculation of the nuclear heat levels in the inner legs of the TF coils, and the need to operate with plasma nuclear powers ranging from 360 (in steady state) to 700MW (pulsed for about 200s), have lead to modifications in the thermal 'screen' on the inside of the case and the size of the conductor cooling channel. The thermal screen removes about 50% of the nuclear heat in the coil with a low temperature rise in the cooling helium and a low pressure drop. The conductor cooling removes the rest, but has a higher pumping power. Optimisation balances the heat removal in the two circuits while keeping minimum pump power.

There have also been adjustments to the specifications on the gaps between the blanket segments that are needed for assembly [4], with a design re-assessment leading to 1-1.5cm instead of 2cms. The reference plasma (500MW) can now be operated with 400s and a 2/hour pulse rate allowing for a 33% uncertainty in the nuclear calculations. An uncertainty up to 100% can be included by a reduction in the 2/hour pulse rate (or an increase in the cryoplant capacity) and higher helium cooling rates, as shown in Table 1 (noting from Fig 6 that the magnet AC losses and eddy currents are about twice the nuclear heating and are also reduced by reducing the pulse rate, giving a rapid offset for the increased nuclear heat) .
The change in blanket gaps also reduces the radiation dose on the TF coil insulation to a peak of 6×10^6 Gy including the full uncertainty factor of 2, compared to the specification of 10^7 Gy.

Recent irradiation testing of insulation samples [5] shows the need to strictly control the composition of DGEBA-type epoxy in order to achieve 10^7 Gy (which will be included into the procurement specifications) and has also identified cyanate-ester blended resins, suitable of vacuum impregnation and with higher bonding strength, that would give resistance possibly up to 5 10^7 Gy. The industrial scale application of these has yet to be investigated, and their use would require acceptance by all parties involved in the construction.

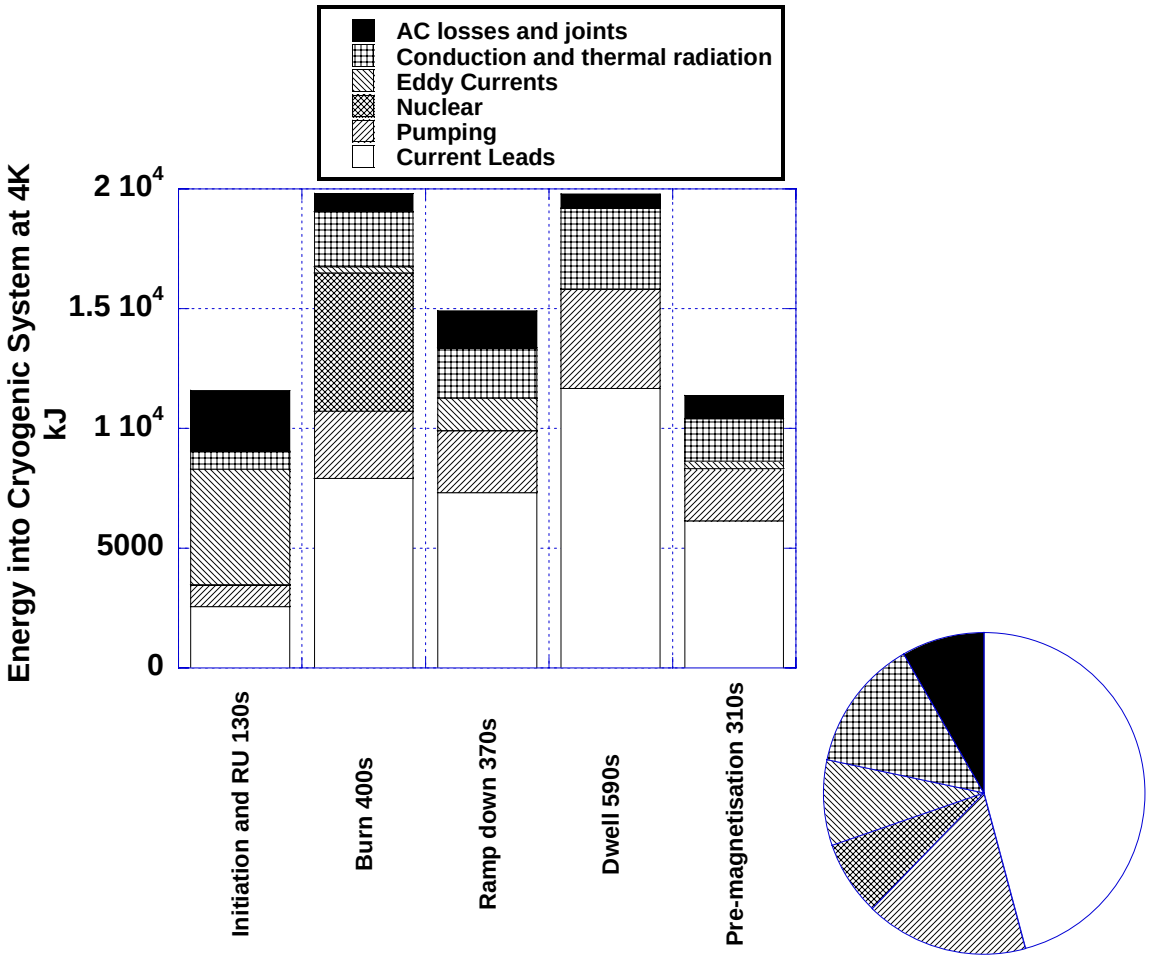

Fig 6 Contributions to Cryoplant Load and Distribution Over 1800s Reference Pulse with 500MW nuclear power (current leads He consumption converted to Joules with 1l/hr=6W)

TABLE 1: SUMMARY OF NUCLEAR HEAT LOADS AND FLEXIBILITY OF COOLING

	Normal Operation (allow 33% margin on nuclear heat)	Operation with 100% Excess Nuclear Heat
Total nuclear heat (during burn) kW	13.9	18
Mass flow rate in TF thermal screen/ winding kg/s	2 /4.5	3 /6
TF pump heating power, 70% efficiency, kW, thermal screen /winding	1.0 /2.6	2.2 /5.6
Pulse rate to maintain constant average heat load	1 every 30 mins	1 every 45 mins

In addition to the already highly variable heat loads shown in Fig 6 for the reference pulses, operation ranging from those due to pulsed high power plasmas with burns of about 100s to lower power steady state operation produces even larger variations. The cryoplant will not remain stable if such loads are transmitted directly. Loads to the cryoplant are smoothed using

the thermal inertia of the magnets and control of the rate of heat extraction, to minimise the constraints on the rate of plasma pulsing. The circuit is illustrated in Fig 7. This smoothing is important during operation with variable length pulses and unexpected heat loads from disruptions, requiring a matching of the pulse rate to the recooling of the magnet system [6].

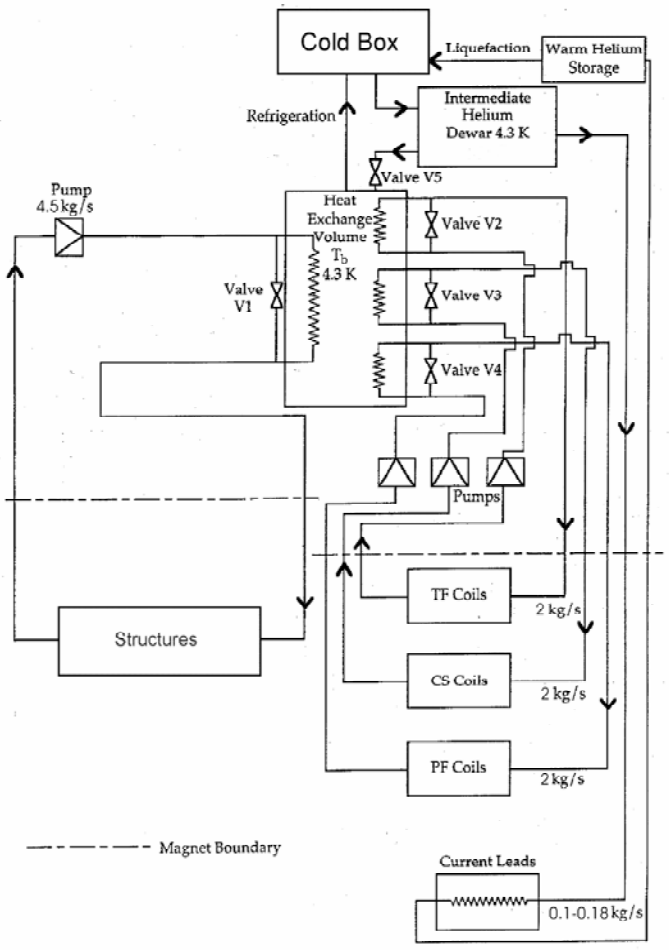

Fig 7 Primary Helium Circuit for the ITER Magnets, Including Bypass Valves and the Current Leads (Valves V2, V3, V4 may not be required)

5. Plasma Shaping and Control

On the electromagnetic design aspects of the coils, in addition to the shaping and vertical plasma stabilisation now provided by the PF coils, the side CC (Fig 8) have been modified with improved cooling and higher operating voltages to extend the Resistive Wall Mode, RWM, stabilisation capability. The CCs also provide error field correction (up to n,m=3 modes), with the coil capacity selected on the basis of the maximum expected errors in manufacture and positioning of the TF, CS and PF coils [7]. To obtain the maximum possible cooling capacity, the conductor has been modified to include a central cooling channel, allowing a mass flow rate of 4g/s at the supply pressure drop of 0.5bar

6. Conclusions

In the 3 years since the end of the ITER EDA, significant progress has been made in finalising the magnet design so that proper procurement specifications can be prepared. The results from the latest R&D (for example, on strand, conductor, nuclear radiation of insulation and structural materials) have been assessed and corresponding design modifications made. On-

going items include the pre-compression rings for the TF coils (fabrication feasibility using uniaxial glass fibre), the TF radial plates (achievable manufacturing tolerances) and the NbTi PF conductor performance. Some design work (especially on stress analysis and thermohydraulic simulations) remains to be done but overall the magnets are ready for the start of the construction phase of ITER.

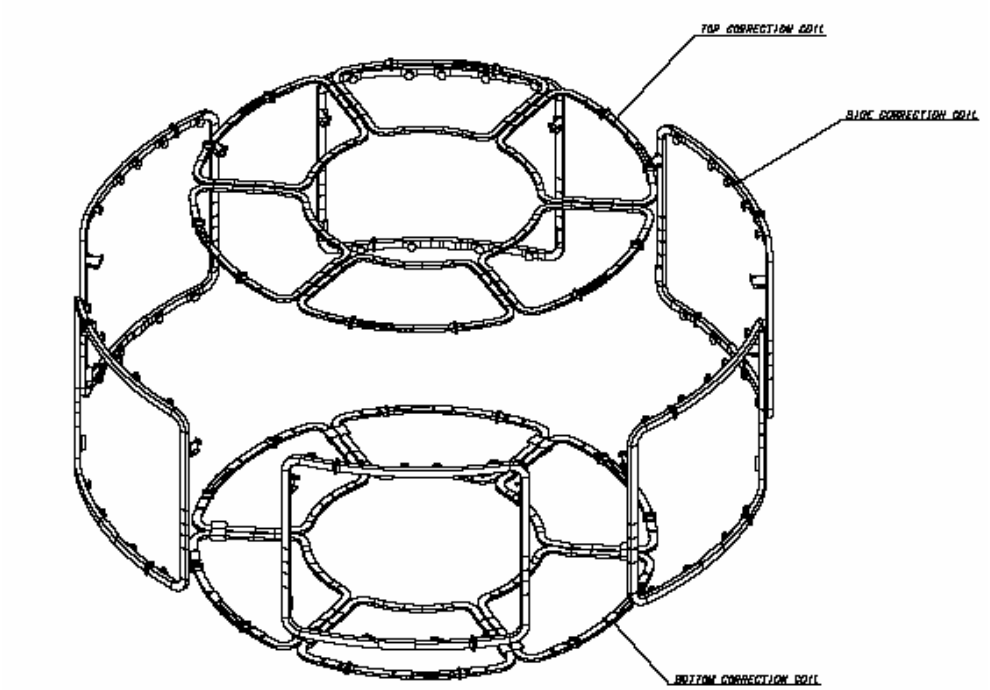

Fig 8 Layout of the Correction Coils, for Error Field Correction and RWM Control

7. References

[1] Magnet Design Description Document (DDD1.1-1.3), Aug 2004, ITER internal report

[2] N. Martovetsky, P. Bruzzone, B. Stepanov, R. Wesche, C.Y. Gung, M. Takayasu; L. Goodrich, A. Nijhuis, Effect of the conduit material on CICC performance under high cycling loads, 18th Applied Superconductivity Conference, Jacksonville, USA, Oct 2004

[3] M. C. Jewell, P. J. Lee, D. C. Larbalestier, The Influence of Nb3Sn Strand Geometry on Filament Breakage under Bend Strain as Revealed by Metallography, Supercond. Sci. Technol. 16 (2003) 1005–1011

[4] H. Iida, L. Petrizzi, V. Khripunov, G. Federici, E. Polunovskiy, Nuclear Analysis of Some Key Aspects of the ITER Design with Monte Carlo Codes, paper presented at 23 Symposium of Fusion Technology, Venice, Sept 2004

[5] K. Bittner-Rohrhofer, K. Humer, H. Fillunger, R.K. Maix, Z. D. Wang, H.W. Weber, Influence of reactor irradiation on the mechanical behaviour of ITER TF coil candidate insulation systems, Fus Eng Des 66-68C (2003), 1201-1207.

[6] N. Mitchell, Simulations of the Operational Control of a Cryogenic Plant for a Superconducting Burning Plasma Experiment, Fusion Engineering and Design, vol 54 (2001), Feb, p97-116.

[7] V. Amoskov, A. Belov, V. Belyakov, O. Filatov, Yu Gribov, E. Lamzin, N. Maixmenkova, B. Mingalev, S. Sytchevsky, Statistical Analysis of Expected Error Fields in Tokamaks and their Correction, to be published in Plasma Devices and Operation, publishers Taylor and Francis, 2004